

## Dry and wet air-side performance of a louver-finned heat exchanger having flat tubes<sup>†</sup>

Nae-Hyun Kim<sup>1,\*</sup> and Soo-Hwan Kim<sup>2</sup>

<sup>1</sup>Department of Mechanical Engineering, University of Incheon #12-1, Songdo-Gu, Yeonsu-Gu, Incheon, 406-840, Korea

<sup>2</sup>Graduate School, University of Incheon #12-1, Songdo-Gu, Yeonsu-Gu, Incheon, 406-840, Korea

(Manuscript Received December 22, 2009; Revised February 9, 2010; Accepted February 26, 2010)

### Abstract

A louver-finned flat tube heat exchanger was tested, and the data are compared with those of the state-of-the-art round tube heat exchanger. Both heat exchangers have the same tube perimeter and fin pitch. Tests were conducted under dry and wet condition. Results show that, under dry condition, both  $j$  and  $f$  factors of the round tube heat exchanger are larger than those of the flat tube heat exchanger. As the Reynolds number decreases, however, the  $j$  and  $f$  factors of the flat tube heat exchanger increase at steeper slopes than those of the round tube heat exchanger. Under wet condition, contrary to the dry surface, both  $j$  and  $f$  factors of the flat tube heat exchanger are larger than those of the round tube heat exchanger. Explanation is provided considering the condensate drainage between louvers and fins. Performance evaluation was also performed.

*Keywords:* Finned tube; Heat exchanger; Dehumidification; Heat transfer coefficient; Pressure drop

### 1. Introduction

Finned-tube heat exchangers having round tubes have been widely used in heat exchange between a liquid and a gas. In the forced convective heat transfer between liquid and gas, the controlling thermal resistance is on the gas-side. To improve the gas-side performance, rigorous efforts have been devoted, which include usage of high performance fins, usage of small diameter tubes, etc. [1-3]. However, finned-tube heat exchangers having round tubes have inherent shortcomings, such as form drag on the tubes, low heat transfer region on the fin behind tubes, etc. These drawbacks may be alleviated if low profile flat or oval tubes are used. Flat tube heat exchangers also have a drawback. They may not withstand a high internal pressure and may deform at a high pressure.

Brauer [4] was the first to investigate the possibility of non-circular finned tubes. He tested staggered banks of oval and round individually finned tubes having 312 fin/m and 10 mm fin height. The oval tubes yielded 15% higher heat transfer coefficient and 25% less pressure drop than round tubes. He attributed the performance advantage of oval tubes to lower form drag on the tubes and the smaller wake region on the fin behind the tubes. Saboya and Saboya [5] applied a naphtha-

lene sublimation technique to measure the mass transfer coefficient in a channel simulating plate fin and oval tube exchanger, and compared the results with those of the round tube counterpart. Two oval tube geometries with 1.54 and 2.0 aspect ratios were tested. No major difference in mass transfer coefficients between round and oval tubes was reported.

Min and Webb [6] numerically investigated the effect of tube aspect ratio of an oval tube on air-side heat transfer and pressure drop characteristics of an infinite row heat exchanger having herringbone wave fins. The numerical calculations were performed in three dimensions for two frontal air velocities, 2.54 and 3.39 m/s, yielding hydraulic diameter Reynolds number of 770 and 1150. Investigated were five tube geometries including a round tube, three oval tubes and a flat tube. The longitudinal and transverse tube pitches were 31.75 mm and 30.48 mm. The corrugation height and corrugation pitch of the fin were 1.67 and 10.58 mm. The fin pitch was 2.117 mm. The 15.88 mm round tube served as a baseline tube. The four non-circular tubes were made by reforming the baseline round tube, and had the same perimeter as that of the round tube. The aspect ratios of the three oval tubes were 2.0, 3.0, 4.29, and the aspect ratio of the flat tube was 3.0. As the tube aspect ratio increased, the air-side heat transfer coefficient and pressure drop decreased. At 2.54 m/s frontal velocity, the 3.0 aspect ratio oval tube yielded a 9.0% lower heat transfer coefficient and a 48.7% lower pressure drop than the round tube. As compared to the 3.0 aspect ratio oval tube, the same aspect

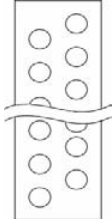

<sup>†</sup> This paper was recommended for publication in revised form by Associate Editor Man-Yeong Ha

\*Corresponding author. Tel.: +82 32 770 8420, Fax: +82 32 770 8410

E-mail address: knh0001@incheon.ac.kr

© KSME & Springer 2010

Table 1. Specifications of round tube and flat tube heat exchanger.

	Round tube	Flat tube
Shape		
Row	2	1
Tube size	7.0mm dia.	3.5mm×9.5mm
Fin pitch	1.4mm	1.4mm
Transverse tube pitch	21.0 mm	17.0 mm
Longitudinal tube pitch	12.7 mm	22.0 mm
Fin thickness	0.10 mm	0.14 mm
Tube thickness	0.32 mm	0.50 mm
Fin pattern	louver	louver
Sample frontal size	398mm ×295mm	398mm ×308mm

ratio flat tube yielded a 2.3% higher heat transfer coefficient and 6.0% higher pressure drop.

Leu et al. [7] also numerically investigated the effect of tube aspect ratio of an oval tube for a two-row heat exchanger having louvered fins. The longitudinal and transverse tube pitches were 19.05 mm and 25.4 mm. The louver pitch was 3.75 mm and the louver angle was 14 degree. The 10.42 mm round tube served as a baseline tube, and the oval tubes had the same perimeter as that of the round tube. The aspect ratios of the oval tubes were varied from 1.2 to 2.8. The numerical calculations were performed for hydraulic diameter Reynolds number from 70 to 370. Results showed that, same as Min and Webb [6], the air-side heat transfer coefficient and pressure drop decreased as the tube aspect ratio increased. The 2.8 aspect-ratio oval tube yielded a 10% lower heat transfer coefficient and a 41% lower pressure drop than the round tube.

Webb and Iyengar [8] compared the air-side performance of a 1024 fins/m louver finned two-row oval tube heat exchanger with that of a two-row finned tube heat exchanger having 8.0 mm round tubes and convex louvered fins at 807 fins/m, tested by Wang et al. [9]. The oval tubes had 5.0 x 8.0 mm cross section, and were arranged in-line with 16 mm transverse pitch. Operating at the same velocity, the comparison revealed that heat transfer coefficients of the oval tube were approximately the same as those of the round tube and pressure drops of the oval tube were 10% lower than those of the round tube. However, information on the air-side performance of the oval geometry was limited due to proprietary reasons.

The above literature survey reveals that almost no investigation is available on the experimental heat transfer and pressure drop data of a finned-tube heat exchanger having oval (or flat) tubes. In this study, a louver-finned heat exchanger having flat tubes was tested, and the results were compared with those of the state-of-the-art louver-finned heat exchanger having round tubes. The flat tube had the same perimeter as the round tube.

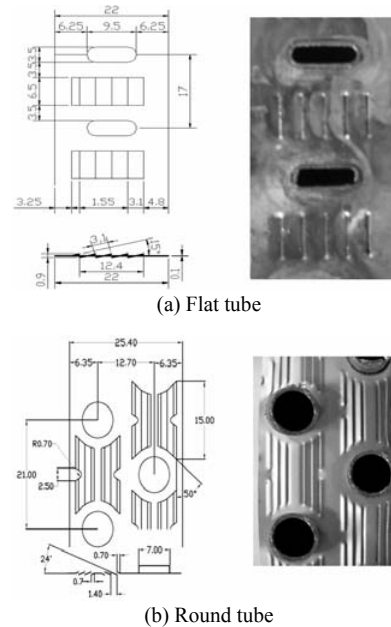


Fig. 1. Heat exchanger geometry.

Tests were conducted under dry and wet surface conditions.

## 2. Experiments

### 2.1 Heat exchanger samples

Geometric details of the flat tube heat exchanger are listed in Table 1. The flat tube heat exchanger has a single row with 17.0 mm transverse tube pitch. Flow depth is 22.0 mm, and fin pitch is 1.4 mm. Details of the flat tube and the fin configuration are shown in Fig. 1. The flat tube was made from a circular tube having a 7.0 mm outer diameter, and the cross-sectional dimension was 9.5 mm x 3.5 mm. Four unidirectional louvers with 3.1 mm louver pitch, 6.5 mm louver length and 15 degree louver angle are formed on the fin. The width and height of the heat exchanger are 398 mm and 308 mm. The round tube heat exchanger has two tube rows with 21.0 mm transverse tube pitch and 12.7 mm longitudinal tube pitch. Flow depth is 25.4 mm, which is 15% larger than that of the flat tube heat exchanger. The tube outer diameter is 7.0 mm, the perimeter of which is the same as that of the flat tube. Fin pitch is 1.4 mm, which is the same as that of the flat tube heat exchanger. X-patterned louvers with 1.4 mm louver pitch, 24 degree louver angle are formed on the fin as shown in Fig. 1. One thing to note is that both heat exchangers have approximately the same air-side heat transfer area. The air-side heat transfer area of the flat tube heat exchanger is 94% that of the circular tube heat exchanger. For both heat exchangers, fins were not hydrophilic treated. Tube inner surfaces were smooth for both heat exchangers, and the tubes were circuited to cross-counter configuration with single inlet and outlet.

Of particular interest of the flat or oval tube heat exchanger is the internal pressure limit, outside which the heat exchanger deforms or bursts. Separate pressure tests were conducted for

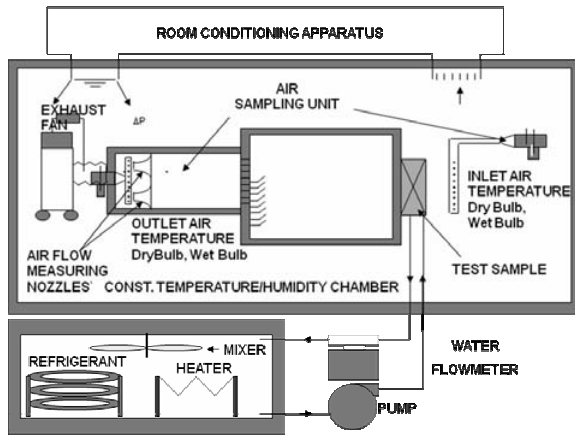


Fig. 2. Schematic of the apparatus.

the present flat tube heat exchanger, through which the deformation and the burst pressure turned out to be 35 bar and 50 bar, respectively. Webb and Iyengar [8] report the design pressures of a refrigerant condenser, which are 24 bar for R134a, 34 bar for R22 and 49 bar for R410A. Thus, the present flat tube heat exchanger may be used for a refrigerant condenser, although safety margins may not be enough.

**2.2 Test apparatus and procedures**

A schematic drawing of the apparatus is shown in Fig. 2. It consists of a suction-type wind tunnel, water circulation and control units, and a data acquisition system. The apparatus is situated in a constant temperature and humidity chamber. The air-side inlet condition of the heat exchanger is maintained by controlling the chamber temperature and humidity. The inlet and outlet dry and wet bulb temperatures are measured by the sampling method suggested in ASHRAE Standard 41.1 [10]. Behind the test sample, a diffusion baffle is installed to mix the outlet air. The waterside inlet condition is maintained by regulating the flow rate and the outlet temperature of the constant temperature bath situated outside of the chamber. Both the air and the water temperatures are measured by pre-calibrated RTDs (Pt-100 Ω sensors). Their accuracies are ± 0.1 K. The water flow rate is measured by a mass flow meter, whose accuracy is ± 0.0015 liter/s. The airside pressure drop across the heat exchanger is measured using a differential pressure transducer. The air flow rate is measured using a nozzle pressure difference according to ASHRAE Standard 41.2 [11]. The accuracy of the differential pressure transducers is ± 1.0 Pa. The wind tunnel is equipped with multiple nozzles, and an appropriate one is selected depending on the air velocity.

For dry surface tests, the water inlet temperature was held at 50°C and the chamber temperature was maintained at 21°C with 60% relative humidity. For wet surface tests, the water inlet temperature was held at 6°C and the chamber temperature was maintained at 27°C with 80% relative humidity. The high relative humidity was needed to ensure fully wet surface of the heat exchanger. Experiments were conducted varying

Table 2. Experimental uncertainties.

Parameter	Max. Uncertainties
Temperature	± 0.1 °C
Differential pressure	± 1 Pa
Water flow rate	± 1.5×10 <sup>-6</sup> m <sup>3</sup> /s
Re <sub>Dh</sub>	± 2%
f	± 10%
j	± 12%

the frontal air velocity from 0.5 m/s to 3.0 m/s. The energy balance between the air-side and the tube-side was within ± 2% for the air velocity larger than 1.0 m/s. It was increased to ± 5% at the air velocity of 0.5 m/s. All the data signals were collected and converted by a data acquisition system (a hybrid recorder). The data were then transmitted to a personal computer for further manipulation. An uncertainty analysis was conducted following ASHRAE Standard 41.5 [12], and the results are listed in Table 2. The major uncertainty on the friction factor was the uncertainty of the differential pressure measurement (± 10%), and the major uncertainty on the heat transfer coefficient (or j factor) was that of the tube-side heat transfer coefficient (± 10%). The uncertainties decreased as Reynolds number increased.

**2.3 Data reduction**

**2.3.1 Dry surface**

Total heat transfer rate used for the calculation of airside heat transfer coefficient was obtained from the average of Q<sub>o</sub> and Q<sub>i</sub>.

$$Q = (Q_o + Q_i) / 2 \tag{1}$$

$$Q_o = \dot{m}_{air} c_{pa} (T_{air,out} - T_{air,in}) \tag{2}$$

$$Q_i = \dot{m}_w c_{pw} (T_{w,in} - T_{w,out}) \tag{3}$$

The tube-side of the two-row round tube heat exchanger is circuited cross-counter, and UA value is obtained from the following equations [13].

$$UA = (\dot{m} c_p)_{air} NTU_2 \tag{4}$$

$$NTU_2 = -2 \ln(1 - K) \tag{5}$$

The K is obtained from the following equations.

$$\frac{K}{2} + (1 - \frac{K}{2}) \exp(2KR) = \frac{1}{1 - RP} \tag{6}$$

$$P = \frac{T_{air,out} - T_{air,in}}{T_{w,in} - T_{air,in}} \tag{7}$$

$$R = \frac{T_{w,in} - T_{w,out}}{T_{air,out} - T_{air,in}} \tag{8}$$

For the one-row flat tube heat exchanger, a cross-flow ε - NTU equation is appropriate. The airside heat transfer coefficient h<sub>o</sub> is then calculated by subtracting the water-

side and wall resistances from the total thermal resistance.

$$\frac{1}{\eta_o h_o A_o} = \frac{1}{UA} - \frac{1}{h_i A_i} - \frac{t}{k_i A_i} \quad (9)$$

where  $\eta_o$  is the overall surface efficiency of heat exchanger, “ $t$ ” is the thickness of tube wall, and subscripts “ $o$ ” and “ $i$ ” stand for air and tube sides, respectively. The tube-side heat transfer coefficient  $h_i$  is evaluated from the Gnielinski [14] semi-empirical correlation.

$$h_i = \left( \frac{k_i}{D_{h,i}} \right) \frac{(\text{Re}_{D_{h,i}} - 1000) \text{Pr}_i (f_i / 2)}{1.0 + 12.7 \sqrt{f_i / 2} (\text{Pr}_i^{2/3} - 1)} \quad (10)$$

where

$$f_i = [1.58 \ln(\text{Re}_{D_{h,i}} - 3.28)]^{-2} \quad (11)$$

For an accurate assessment of the airside heat transfer coefficient, it is important to minimize the tube-side thermal resistance. Throughout the experiment, the tube-side thermal resistance was less than 10% of the total thermal resistance.

The surface efficiency  $\eta_o$  is obtained from Eq. (12).

$$\eta_o = 1 - \frac{A_f}{A_o} (1 - \eta) \quad (12)$$

For the two-row round tube geometry, the fin efficiency is given by Schmidt [15] as

$$\eta = \frac{\tanh(m r_c \phi)}{m r_c \phi} \quad (13)$$

where

$$m = \sqrt{\frac{2h_o}{k_f t_f}} \quad (14)$$

$$\phi = \left( \frac{R_{eq}}{r_c} - 1 \right) \left[ 1 + 0.35 \ln \left( \frac{R_{eq}}{r_c} \right) \right] \quad (15)$$

$$\frac{R_{eq}}{r_c} = 0.635 \frac{P_t}{r_c} \left( \frac{\sqrt{(P_t/2)^2 + P_t^2}}{P_t/2} - 0.3 \right)^{0.5} \quad (16)$$

For the one-row flat-tube geometry, the oval-tube fin efficiency equation given by Min et al. [16] was used. Their equation has a similar form as Schmidt's equation [15]. Same Eqs. (13), (14) and (15) are applicable with

$$\frac{R_{eq}}{r_c} = e^{\frac{c}{2.3} - 1} [0.855 + e^{-2.15x} + \ln^{0.72}(x + 3)] \quad (17)$$

In Eq. (17), “ $x$ ” is the ratio of the major and minor diameter of the oval (or flat) tube, and “ $c$ ” is the ratio of outer and inner perimeter of equivalent circular fin. The “ $c$ ” is obtained from

$$c = 2\pi R_{eq} / C \quad (18)$$

$$C = \pi[1.5(a + b) - \sqrt{ab}] \quad (19)$$

$$R_{eq} = 0.64 P_t \left( \frac{P_t}{P_i} - 0.2 \right)^{0.5} \quad (20)$$

In Eq. (19), “ $a$ ” is a major and “ $b$ ” is a minor dimension of the flat tube. With Eqs. (12) to (20), an iterative procedure is needed to obtain the airside heat transfer coefficient  $h_o$ . The heat transfer coefficient is traditionally presented as the Colburn  $j$  factor. As for the Reynolds number, a hydraulic-diameter-based Reynolds number was used.

$$\text{Re}_{Dh} = \frac{V_{\max} D_h}{\nu} \quad (21)$$

$$j = \frac{h_o}{\rho_o V_{\max} c_{p_o}} \text{Pr}_o^{2/3} \quad (22)$$

In Eqs. (21) and (22),  $V_{\max}$  is the maximum velocity in the core of the heat exchanger. All the fluid properties were evaluated at an average air temperature. The core friction factor is calculated from the measured pressure drop.

$$f = \frac{A_c \rho_m}{A_o \rho_{in}} \left[ \frac{2\Delta P \rho_{in}}{(\rho_m V_{\max})^2} - (1 + \sigma^2) \left( \frac{\rho_{in}}{\rho_{out}} - 1 \right) \right] \quad (23)$$

In Eq. (23), the entrance and the exit loss coefficients are neglected following the suggestion by Wang et al. [17].

### 2.3.2 Wet surface

Eq. (1) is used to calculate the average heat transfer rate, with the air-side heat transfer rate obtained from the enthalpy difference between the inlet and the outlet.

$$\dot{Q}_o = \dot{m}_{air} (i_{air,oot} - i_{air,in}) \quad (24)$$

For the wet surface analysis of two-row round tube heat exchanger, Eqs. (4)-(8) are applicable with the following modifications.

$$UA = (\dot{m})_{air} NTU_2 \quad (25)$$

$$NTU_2 = -2 \ln(1 - K) \quad (26)$$

The  $K$  is obtained from the following equations.

$$\frac{K}{2} + \left( 1 - \frac{K}{2} \right) \exp(2KR) = \frac{1}{1 - RP} \quad (27)$$

$$R = \frac{i_{w,in} - i_{w,out}}{i_{air,out} - i_{air,in}} \quad (28)$$

$$P = \frac{i_{air,out} - i_{air,in}}{i_{w,in} - i_{air,in}} \quad (29)$$

The effectiveness and NTU definitions for wet surface analysis of one-row flat tube heat exchanger are as follows [18].

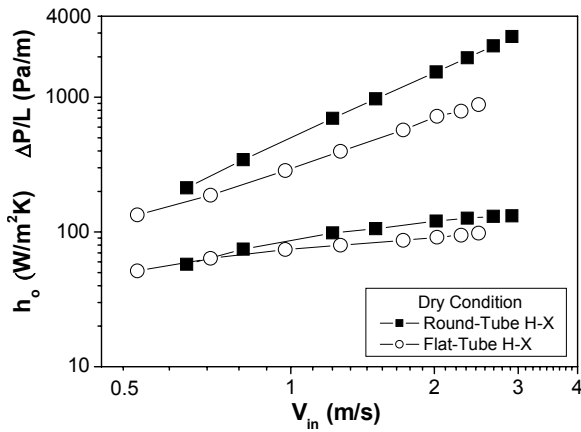


Fig. 3. Air-side heat transfer coefficient and pressure drop per unit depth of the two heat exchangers under dry condition as a function of frontal air velocity.

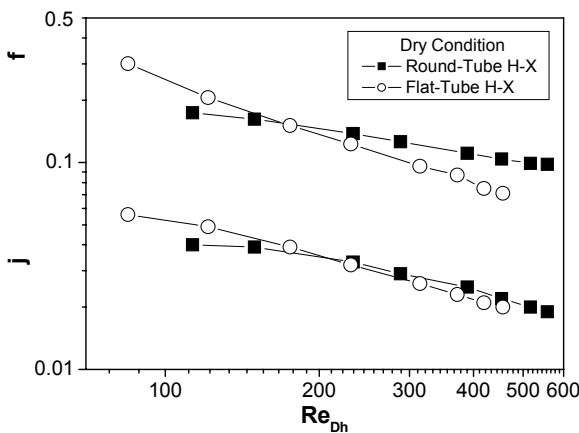


Fig. 4. Air-side j and f factors of the two heat exchangers under dry condition as a function of Reynolds number.

$$\varepsilon = \frac{Q}{C_{\min}(i_{air,in} - i_{w,in})} \tag{30}$$

$$C_r = \frac{C_{\min}}{C_{\max}} = \frac{\min[\dot{m}_{air}, (\dot{m}_w c_{pw} / b_{r12})]}{\max[\dot{m}_{air}, (\dot{m}_w c_{pw} / b_{r12})]} \tag{31}$$

The UA value is obtained from the following equation.

$$UA = C_{\min} NTU \tag{32}$$

The wet surface heat transfer coefficient  $h_{ow}$  is then calculated by subtracting the water-side and wall resistances from the total thermal resistance.

$$\frac{b_{wm}}{\eta_o h_{ow} A_o} = \frac{1}{UA} - \frac{b_r}{h_i A_i} - \frac{b_{pt}}{k_t A_t} \tag{33}$$

The values  $b_r$ ,  $b_{pt}$ , and  $b_{wm}$  in Eq. (33) are the slopes of the saturated air enthalpy – temperature curves at the mean coolant temperature, the mean tube wall temperature and the mean water film temperature on the air-side surface, respectively. The sensible heat transfer coefficient  $h_o$  is finally

obtained from the wet surface heat transfer coefficient  $h_{ow}$  using the following relationship [18].

$$h_o = \left( \frac{c_{pa}}{b_{wm} h_{ow}} \right) \tag{34}$$

For the wet surface fin efficiency, Eqs. (12)-(20) are applicable with modification of Eq. (14) to Eq. (35).

$$m = \sqrt{\frac{2h_{ow}}{k_f t_f}} \tag{35}$$

The wet surface j factor [Eq. (22)] is determined from the sensible heat transfer coefficient  $h_o$ .

### 3. Results and discussions

#### 3.1 Dry surface

Fig. 3 shows the test results under dry condition. The ordinates are heat transfer coefficient  $h_o$  and pressure drop per unit depth  $\Delta P/L$ , while the abscissa is the frontal velocity. At high frontal velocities,  $h_o$  and  $\Delta P/L$  of the round-tube heat exchanger are significantly larger than those of flat-tube heat exchanger. At a frontal velocity 2.5 m/s, for example,  $h_o$  of the round tube heat exchanger is 31% larger than that of the flat tube heat exchanger, and  $\Delta P/L$  of the round tube heat exchanger is 147% larger than that of the flat tube heat exchanger. As the velocity decreases, however,  $h_o$  and  $\Delta P/L$  of the round tube heat exchanger decrease at steeper slopes than those of the flat-tube heat exchanger, yielding approximately the same values at 0.5 m/s (when round tube data are extrapolated to 0.5 m/s). The difference in the slope suggests that heat transfer and friction characteristics of the two heat exchangers are different. This point will be elaborated in the following paragraph. The surface efficiencies were calculated, which yielded 83 to 91 % for the round tube heat exchanger, and 75 to 84 % for the flat tube heat exchanger. The surface efficiency decreased as the frontal velocity increased.

The j and f factors of the two heat exchangers are shown in Fig. 4 as a function of hydraulic-diameter-based Reynolds number. Fig. 4 shows that, at high Reynolds numbers, both j and f factors of the round tube heat exchanger are larger than those of the flat tube heat exchanger. At the Reynolds number 450, for example, the j factor of the round tube heat exchanger is 10% larger than that of the flat tube heat exchanger, and the f factor of the round tube heat exchanger is 46% larger than that of the flat tube heat exchanger. As the Reynolds number decreases, however, the j and f factors of the flat tube heat exchanger increase at steeper slopes than those of the round tube heat exchanger, yielding higher values at low Reynolds numbers. The cross-over Reynolds numbers are approximately 170 for the f factor and 200 for the j factor.

The characteristic geometry of the flat tube heat exchanger may be thought to be a flat plate, where Reynolds number

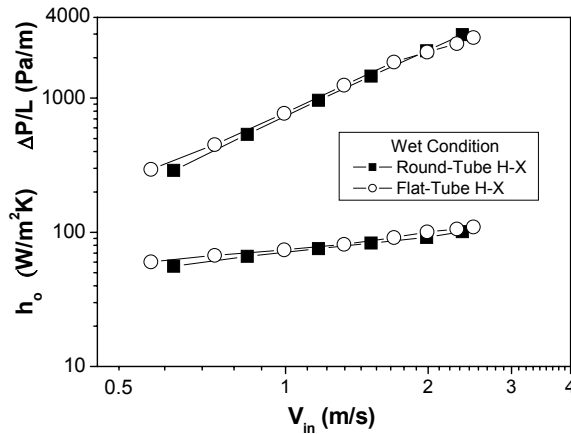


Fig. 5. Air-side heat transfer coefficient and pressure drop per unit depth of the two heat exchangers under wet condition as a function of frontal air velocity.

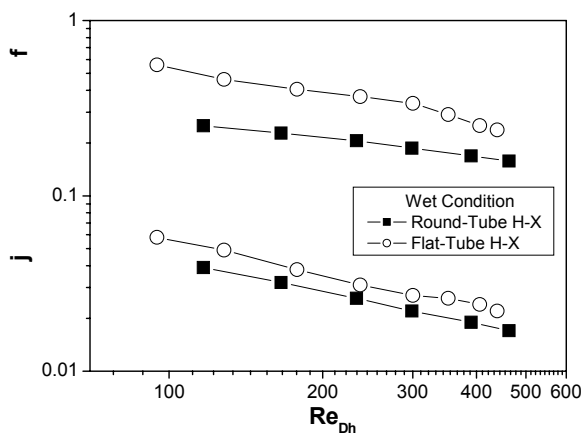


Fig. 6. Air-side  $j$  and  $f$  factors of the two heat exchangers under wet condition as a function of Reynolds number.

exponents are  $-0.5$  both for  $j$  and  $f$  factors [19]. On the other hand, the characteristic geometry of the round tube heat exchanger may be thought to be a combination of flat plate and cylinders. The Reynolds number exponents of a cylinder at the present tube-diameter-based Reynolds number range (which is  $500 \sim 2000$ ) are  $-0.5$  for  $j$  factor and  $-0.23$  for  $f$  factor [19]. Thus, it is expected that Reynolds number exponents of the  $j$  factors are approximately the same for both heat exchangers, whereas the Reynolds number exponent of the  $f$  factor is larger for the flat tube heat exchanger. Fig. 4 indeed shows the expected trend. Reynolds number exponents of the flat tube heat exchanger were  $-0.64$  for the  $j$  factor and  $-0.83$  for the  $f$  factor, and the exponents of the round tube heat exchanger were  $-0.48$  for  $j$  and  $-0.38$  for  $f$ .

### 3.2 Wet surface

Test results under wet condition are shown in Fig. 5. The flat tube heat exchanger yields higher  $h_o$  and  $\Delta P/L$ , although the difference is not significant. This result is in contrast to the dry surface, where  $h_o$  and  $\Delta P/L$  were higher for the round-tube heat exchanger. Fig. 5 shows that the  $h_o$  of

the flat tube heat exchanger are 6-8% higher than those of the round tube heat exchanger. The  $\Delta P/L$  of the flat tube heat exchanger are 3-5% higher, although the trend is reversed at high frontal velocities. The wet surface efficiencies were calculated, which yielded 69 to 81 % for the round tube heat exchanger, and 47 to 63 % for the flat plate heat exchanger. In general, fin efficiency is lower under wet condition than under dry condition because the wet surface heat transfer coefficient  $h_{ow}$  is larger than the dry surface heat transfer coefficient  $h_o$ .

The  $j$  and  $f$  factors under wet condition are shown in Fig. 6 as a function of Reynolds number. Fig. 6 shows that both the  $j$  and  $f$  factors of the flat tube heat exchanger are larger than those of the round tube heat exchanger. The  $j$  and  $f$  of the flat tube heat exchanger are 23-29 % and 51-80% larger than those of round tube heat exchanger. This result is in contrast to the dry surface, where round tube heat exchanger yielded higher  $j$  and  $f$  factors, except at low Reynolds numbers. The present wet surface tests were conducted with the heat exchanger surface fully wet with the condensate. In such a case, the condensate drainage characteristics may significantly affect the heat transfer and pressure drop of the heat exchanger. The significant increase of the  $f$  factor for the flat tube heat exchanger and the decrease of  $j$  factor for the round tube heat exchanger may be related to the condensate drainage characteristics of the heat exchanger. This point will be further elaborated in the following paragraph.

Fig. 6 shows that Reynolds exponents of the two heat exchangers are approximately the same (between  $-0.4$  and  $-0.6$ ). Under wet condition, the surface becomes rough with condensate drops or films. This will be especially true for the present untreated surfaces. In such a case, the heat transfer and friction characteristics will be governed by the rough surface and the presence of tubes may not significantly affect the heat transfer and friction characteristics of the heat exchanger. On the other hand, under dry condition, round tubes significantly affected the heat transfer and pressure drop characteristics of the heat exchanger as previously discussed.

The dry and wet surface  $j$  and  $f$  factors of the two heat exchangers are compared in Fig. 7. For the flat tube heat exchanger, the  $j$  factors of the wet surface are approximately the same as those of dry surface. For the round tube heat exchanger, however, wet surface  $j$  factors are 2-23% lower than dry ones. The reason may be attributed to the difference in louver pitch, which is 3.1 mm for the flat tube heat exchanger and 1.4 mm for the round tube heat exchanger. For louvered surfaces under wet condition, condensate may bridge between louvers as identified by McLaughlin and Webb [20]. Under such circumstances, the heat transfer coefficient decreases significantly because the air flow no longer follows louvers and instead passes through the duct formed by fins [1]. It is speculated that this happened to louvered fins of the round tube heat exchanger, which resulted in the decrease of  $j$  factors as compared with those of the dry surface. The fins of the flat tube heat exchanger had large louver pitch of 3.1 mm, and thus, the condensate bridging did not occur, which resulted in

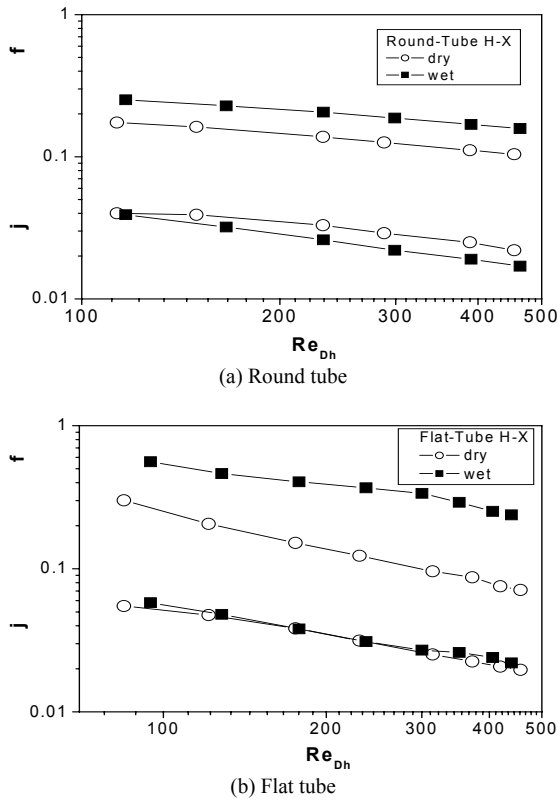


Fig. 7. Air-side  $j$  and  $f$  factors of the two heat exchangers under dry and wet conditions as a function of Reynolds number.

the same  $j$  factors between dry and wet surfaces.

Fig. 7 shows that the  $f$  increase between wet and dry surface is more pronounced for the flat tube heat exchanger as compared with that of the round tube heat exchanger. The increase is 86-235% for the flat tube heat exchanger, and 44-52% for the round tube heat exchanger. The pronounced increase of  $f$  factor for the flat tube heat exchanger may be attributed to the poor condensate drainage characteristics of the flat tube heat exchanger. For the flat tube heat exchanger, flat tubes may retard the smooth down-flow of the condensate, and the accumulated condensate chunks increase the pressure drop. For the round tube heat exchanger, however, the condensate is expected to flow down smoothly. One thing to mention is that the present fins are not hydrophilically treated. Hydrophilic treatment will ease the condensate flow and reduce the pressure drop.

In Fig. 8,  $j/f^{1/3}$  values of the two heat exchangers are plotted as a function of Reynolds number. As described by Webb and Kim [1], the ratio of the air-side performance  $h_o A_o$  (or heat duty) is given by Eq. (36) for the same heat transfer area and pumping power constraints.

$$\frac{(h_o A_o)_f}{(h_o A_o)_r} = \frac{(j/f^{1/3})_f}{(j/f^{1/3})_r} \quad (36)$$

Fig. 8 shows that  $j/f^{1/3}$  values are approximately the same for the two heat exchangers, although slightly better

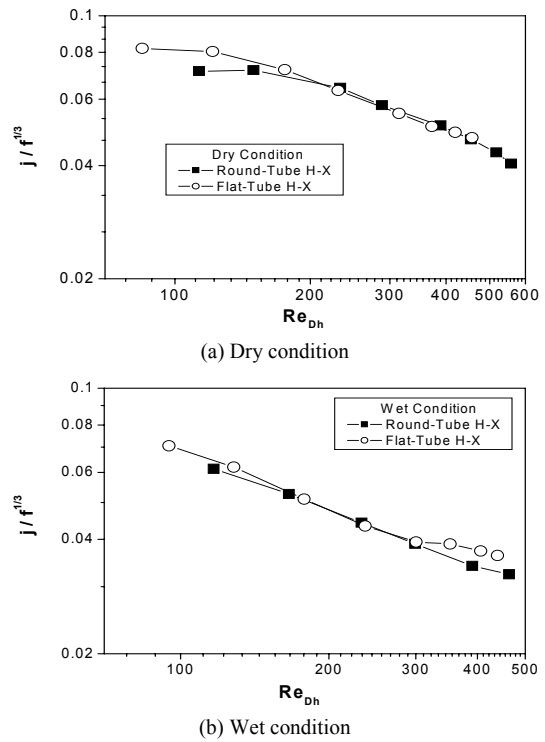


Fig. 8 Air-side performance evaluation ( $j/f^{1/3}$ ) of the two heat exchangers under dry and wet conditions as a function of Reynolds number.

results are identified for the flat tube heat exchanger at low or high Reynolds numbers.

#### 4. Conclusions

Heat transfer and pressure drop data of a one-row flat tube heat exchanger were experimentally obtained, and the data compared with those of the state-of-the-art two-row round tube heat exchanger. For both heat exchangers, the tube perimeter and fin pitch are the same. However, the flow depth of the round tube heat exchanger is 15% larger than that of the flat tube heat exchanger. Tests were conducted under dry and wet condition. Listed below are the major findings.

Under dry condition, both  $j$  and  $f$  factors of the round tube heat exchanger are larger than those of the flat tube heat exchanger, especially at high Reynolds numbers. As the Reynolds number decreases, however,  $j$  and  $f$  factors of the flat tube heat exchanger increase at steeper slopes than those of the round tube heat exchanger, yielding higher  $j$  and  $f$  factors.

Under wet condition, both  $j$  and  $f$  factors of the flat tube heat exchanger are larger than those of the round tube heat exchanger.

For the flat tube heat exchanger, wet surface  $j$  factors are approximately the same as those of a dry surface. For the round tube heat exchanger, however, wet surface  $j$  factors are lower than dry ones, the reason of which may be attributed to the condensate bridging between louvers.

The  $f$  factor increase between wet and dry surface is more pronounced for the flat tube heat exchanger as compared with

that of the round tube heat exchanger. The pronounced increase of  $f$  factor for the flat tube heat exchanger may be attributed to the poor condensate drainage characteristics.

The  $j/j^{1/3}$  values of the two heat exchangers are approximately the same.

## Nomenclature

$a$	: Major dimension of the flat tube (m)
$A$	: Heat transfer area (m <sup>2</sup> )
$b$	: Minor dimension of the flat tube (m)
$b_{r12}$	: Slope of the air saturation curve between the inlet and exit air temperature (J/kg · K)
$b_p$	: Slope of the air saturation curve between the outside and inside tube wall temperature (J/kg · K)
$b_r$	: Slope of the air saturation curve between the mean tube and water temperature (J/kg · K)
$b_{wm}$	: Slope of the air saturation curve at the mean water film temperature of the airside surface (J/kg · K)
$c$	: Ratio of outer and inner perimeter of equivalent circular fin (dimensionless)
$C$	: Tube perimeter (m)
$c_p$	: Specific heat (J/kg · s)
$C_r$	: Heat capacity ratio (dimensionless)
$D_h$	: Hydraulic diameter (m)
$f$	: Airside friction factor (dimensionless)
$f_i$	: Tube-side friction factor (dimensionless)
$h$	: Heat transfer coefficient (W/m <sup>2</sup> · K)
$i$	: Enthalpy (J/kg)
$j$	: Colburn $j$ factor (dimensionless)
$k$	: Thermal conductivity, (W/m · K)
$L$	: Tube depth (m)
$\dot{m}$	: Mass flow rate (kg/s)
$NTU$	: Number of transfer units (dimensionless)
$P_l$	: Longitudinal tube pitch (m)
$P_t$	: Transverse tube pitch (m)
$Pr$	: Prandtl number (dimensionless)
$Q$	: Heat transfer rate (W)
$r_c$	: Tube radius including fin collar (m)
$R_{eq}$	: Equivalent radius (m)
$Re_{Dh}$	: Reynolds number based on $D_h$ (dimensionless)
$t$	: Tube wall thickness (m)
$T$	: Temperature (K)
$t_f$	: Fin thickness (m)
$U$	: Overall heat transfer coefficient (W/m <sup>2</sup> · K)
$V_{max}$	: Velocity based on the minimum flow area of the frontal surface (m/s)

## Greek letters

$\varepsilon$	: Thermal effectiveness (dimensionless)
$\Delta P$	: Pressure loss (Pa)
$\eta$	: Fin efficiency (dimensionless)
$\eta_o$	: Surface efficiency (dimensionless)
$\rho$	: Density (kg/m <sup>3</sup> )
$\nu$	: Kinematic viscosity (m <sup>2</sup> /s)

$\sigma$  : Contraction ratio of the cross-sectional area (dimensionless)

## Subscripts

2	: Subscript of NTU
a	: Air
c	: Heat exchanger core
i	: Tube-side
in	: Inlet
f	: Fin, flat tube
m	: Mean
max	: Maximum
min	: Minimum
o	: Outside
out	: Outlet
r	: Round tube
t	: Tube
w	: Water, wet surface

## References

- [1] R. L. Webb and N.-H. Kim, Principles of Enhanced Heat Transfer, 2<sup>nd</sup> ed., Taylor and Francis Pub. (2005).
- [2] R. Hu and C. C. Wang, A review of fin-and-tube heat exchangers in air-conditioning applications. *Int. J. Air-Cond. Ref.* 15 (2007) 85-100.
- [3] N.-H. Kim, J.-P. Cho, W.-K. Oh, Y.-H. Choi and H. Gaku, Heat transfer and pressure drop characteristics of plain finned heat exchangers having 5.0 mm tubes. *Int. J. Air-Cond. Ref.*, 16 (2008) 9-14.
- [4] H. Brauer, Compact heat exchangers. *Chem. Prog. Eng.*, 45 (8) (1964) 451-460.
- [5] S. M. Saboya and F. E. M. Saboya, Experiments on elliptic sections in one- and two-row arrangements of plate fin and tube heat exchangers. *Exp. Thermal Fluid Science*, 24 (2001) 67-75.
- [6] J.-C. Min and R. L. Webb, Numerical analysis of effects of tube shape on performance of a finned tube heat exchanger. *J. Enhanced Heat Transfer*, 11 (1) (2004) 61-73.
- [7] J.-S. Leu, M.-S., Liu, J.-S. Liaw and C.-C. Wang, A numerical investigation of louvered fin-and-tube heat exchangers having circular and oval tube configurations. *Int. J. Heat Mass Transfer*, 44 (2001) 4235-4243.
- [8] R. L. Webb and A. Iyengar, Oval finned tube condenser and design pressure limits. *J. Enhanced Heat Transfer*, 8 (2001) 147-158.
- [9] C.-C. Wang, Y.-M. Tsai and D.-C. Lu, A comparative study of convex-louver and wavy fin-and-tube heat exchangers. *Exp. Heat Trans.*, 9 (1996) 61-78.
- [10] ASHRAE Standard 41.1-1986. Standard method for temperature measurement. ASHRAE, Atlanta, GA, USA (1986).
- [11] ASHRAE Standard 41.2-1987. Standard method for laboratory air-flow measurement. ASHRAE, Atlanta, GA, USA (1987).
- [12] ASHRAE Standard 41.5-1975. Standard measurement



- guide, engineering analysis of experimental data. ASHRAE, Atlanta, GA, USA (1975).
- [13] J. Taborek,  $F$  and  $\theta$  charts for cross-flow arrangements. Heat Exchanger Design Handbook. Begell House Inc., Section 1.5.3 (1998).
- [14] V. Gnielinski, New equations for heat and mass transfer in turbulent pipe flows. *Int. Chem. Eng.*, 16 (1976) 359-368.
- [15] T. E. Schmidt, Heat transfer calculations for extended surfaces. *J of ASRE, Refrigeration Engineering.*, 4 (1949) 351-357.
- [16] J.-C. Min, T. Tao and X.-F. Peng, Efficiency of fins used in a finned oval tube heat exchanger. *J. Enhanced Heat Transfer*, 10 (3) (2003) 323-334.
- [17] C.-C. Wang, R. L. Webb and K.-Y. Chi, Data reduction for airside performance of fin-and-tube heat exchangers. *Exp. Thermal Fluid Sci.*, 21 (2000) 218-226.
- [18] M.-H. Kim and C. W. Bullard, Airside performance of brazed aluminum heat exchanger under dehumidifying conditions. *Int. J. Refrigeration*, 25 (2002) 924-934.
- [19] F. P. Incropera and D P. Dewitt, Fundamentals of heat and mass transfer. 3<sup>rd</sup> ed., John Wiley and Sons (1990).
- [20] W. J. McLaughlin and R. L. Webb, Condensate drainage and retention in louver fin automotive evaporators. *SAE Technical Paper Series*, 2000-01-0575 (2000).



**Nae-Hyun Kim** is a Professor of Mechanical Engineering, University of Incheon. His area of interest spans boiling and condensation, heat transfer enhancement and heat exchanger design. He has been active in heat transfer community, and was a Chairman of Thermal Engineering Division of KSME. He holds several editorial position including Journal of Enhanced Heat Transfer. He is a recipient of Asian Academic Award awarded by SAREK and JSRAE.